Supplementary Information (SI) for Chemical Communications.
This journal is © The Royal Society of Chemistry 2024

SUPPORTING INFORMATION

Hydrazide-Based Reactive Matrices for the Sensitive Detection of Aldehydes and Ketones by MALDI Mass Spectrometry Imaging

Henrik Lodén [a ‡], Luke S. Schembri [a b ‡], Anna Nilsson [a], Ibrahim Kaya [a], Reza Shariatgorji [a], Luke R. Odell [b *], Per E. Andrén [a *]

[a] Department of Pharmaceutical Biosciences, Spatial Mass Spectrometry, Science for Life Laboratory, Uppsala University, Uppsala, Sweden.

[b] Department of Medicinal Chemistry, Uppsala University, Uppsala, Sweden.

[‡] These authors contributed equally.

[*] Corresponding authors. luke.odell@ilk.uu.se, per.andren@uu.se

Contents

Experimental S1
Chemicals and General Methods S1
Design and Synthesis of Reactive Matrices S1
Animal Experiments and Tissue Preparation S5
MALDI Imaging S6
Synthetic Pathway S8
Compound ^{13}C and ^{1}H NMR Spectra S9
Compound UV Spectra S15
Accurate Mass Determination S16
Model Compound Structures S16
MALDI MSI S17
MS/MS Spectra S19
High-resolution imaging S20
Supporting Tables S21
References S22

Experimental

Chemicals and General Methods

All solvents and chemicals used for the synthesis and preparation of the matrices were of pro-analysis grade and obtained from Merck KGaA (Darmstadt, Germany), Enamine (Kyiv, Ukraine) or Ambeed (Arlington Heights, IL, USA), unless otherwise specified.

Analytical thin-layer chromatography (TLC) was performed on silica gel 60 F-254 plates and visualised with UV light. Flash column chromatography was performed using silica gel 60 (40-63 µm). ^{1}H and $^{13}C\{1H\}$ NMR spectra were recorded at 400 and 101 MHz, respectively. The chemical shifts for ^{1}H NMR and $^{13}C\{1H\}$ NMR were referenced to TMS via residual solvent signals (^{1}H: $CDCl_3$ at 7.26 ppm and DMSO-d_6 at 2.50 ppm; $^{13}C\{1H\}$: $CDCl_3$ at 77.16 ppm and DMSO-d_6 at 39.52 ppm). Analytical HPLC/ESI-MS was performed using electrospray ionisation (ESI) and a C18 column (50×3.0 mm, 2.6 µm particle size, 100 Å pore size) with CH_3CN/H_2O in 0.05 % aqueous HCOOH as the mobile phase at a flow rate of 1.5 mL/min. LC purity analyses were run on a C18 column using a gradient of 5-100 % CH_3CN/H_2O in 0.05 % aqueous HCOOH as the mobile phase at a flow rate of 1.5 mL/min for 5 minutes, unless otherwise stated. High-resolution molecular masses were determined using high-resolution MS (HRMS) on a mass spectrometer equipped with a matrix-assisted laser-desorption ionisation (MALDI) source and a Fourier transform ion cyclotron resonance (FTICR) mass analyser.

Design and Synthesis of Reactive Matrices

The carbonyl-reactive matrices **9a-c** all incorporated a hydrazide reactive group, similar to Girard's T and P reagents [1], located at different distances from the permanent charge of the molecules. The hydrazide functional group is known to selectively and covalently react with the target functional groups under physiological conditions and was considered ideally suited for our purpose [2-5]. Furthermore, addition of polycyclic aromatic anthracene to the matrix-structures was expected to significantly increase the ionisation efficiency, as exemplified in our previous work with FMP based matrices. Besides increasing the laser absorptivity [6], this may also have been due to improved crystallinity of the matrix.

The synthetic pathway for the three matrices is given in Supporting Information Fig. S. Synthesis of all matrices began with coupling of the pyridine ring (**1**) to the strongly UV-absorbent anthracene system (**2**) via a Suzuki coupling to obtain (**3**). It should be noted that, despite the mediocre yield, more material can be obtained via further recrystallisation in acetone. The resulting material is less pure but impurities can easily be removed in the subsequent step. The reactive group was installed through a substitution reaction (S_N2) of **3** with **7b** or **7c** to form **8b** and **8c**, respectively. After this point, the products were relatively unstable and had to be handled carefully to avoid N-alkyl cleavage and reformation of the starting material **3**. Hence, all subsequent products were purified by a series of triturations with various solvents using a centrifuge and sonicator (see Chemicals and General Methods section). Intermediates **8b** and **8c** were formed instead of directly synthesising the final matrix (as per **9a**). Direct synthesis was attempted, but the longer alkyl chains meant that harsher conditions were required for the substitution to take place. Such conditions caused the heat-promoted degradation of the hydrazide tert-butoxycarbonyl (BOC) protecting group (as indicated by an increase in pressure of the closed vessel) and a subsequent substitution reaction of the free hydrazide with the N-alkyl pyridinium group to re-form **3**. Logically, **8c** gave lower yields compared to **8b** due to the longer alkyl chain, resulting in lower reactivity (the temperature again had to be carefully controlled).

As previously mentioned, **9a** could be formed directly from **3** by reacting with **6** in a super-heated reaction in a closed vessel. However, the reaction had to be stopped after 4 hours as signs of BOC degradation were noted. From here, the BOC protecting group was acidolytically removed and the product isolated in good yields as the free base.

Matrices **9b** and **9c** were first converted to their corresponding acid chlorides using oxalyl chloride. These were then directly reacted with **6** to form the BOC-protected matrices, after which the same deprotection method as **9a** afforded the matrices in good yields. Interestingly, **9a** could not be formed in the same way as **9b** and **9c** as the use of oxalyl chloride on "**8a**" led to the formation of an unidentified by-product. Usefully, such a synthetic pathway is amenable to scaling up (or scaling out into several reaction vials) as all workup procedures avoid the use of column chromatography.

4-(anthracen-9-yl)pyridine (3): A stirred solution of 4-pyridylboronic acid **1** (1.74 g, 12.7 mmol, reagent grade 90 %), 9-bromoanthracene **2** (1.26 g, 4.90 mmol) and $Pd(PPh_3)_4$ (173 mg, 0.150 mmol) in toluene/ethanol (4:1, 45 mL) was added to an aqueous saturated solution of Na_2CO_3 (22.5 mL) and stirred at 90 °C for 23 h. After cooling to room temperature, the reaction mixture was extracted with Et_2O (3 x 100 mL). The combined organic layers were dried over $MgSO_4$, filtered and concentrated in vacuo. The filtrate was evaporated to dryness and purified by recrystallisation in hot acetone to give **3** as a cream-colored solid (713 mg, 57 %). ^{1}H NMR ($CDCl_3$) δ 8.88 – 8.81 (m, 2H), 8.55 (s, 1H), 8.10 – 8.04 (m, 2H), 7.59 – 7.54 (m, 2H), 7.52 – 7.47 (m, 2H), 7.43 – 7.37 (m, 4H).; ^{13}C{1H}NMR (CDCl3) δ 150.1, 147.7, 133.7, 131.4, 129.5, 128.7, 127.8, 126.7, 126.2, 126.0, 125.5.

tert-butyl 2-(2-chloroacetyl)hydrazine-1-carboxylate (6): To a stirred and cooled (0 °C) solution of tert-butyl hydrazinecarboxylate **5** (1.98 g, 15 mmol) in dichloromethane (DCM, 20 mL) and pyridine (0.79 g, 10 mmol), chloroacetyl chloride **4** (1.12 g, 10 mmol) in DCM (5 mL) was added. The reaction mixture was stirred for 6 h and then washed with diluted HCl (3 × 50 mL). The organic phase was dried over Na_2SO_4. The solvent was removed under reduced pressure to yield **6** as a clear oil that solidified on standing (1.16 g, 55 %). ^{1}H NMR ($CDCl_3$) δ 8.27 (s, 1H), 6.60 (s, 1H), 4.12 (s, 2H), 1.48 (s, 9H). ^{13}C{1H}NMR ($CDCl_3$) δ 165.3 154.9, 82.4, 41.1, 28.1.

3-(4-(anthracen-9-yl)pyridin-1-ium-1-yl)propanoate (8b): **3** (318 mg, 1.25 mmol) and 3-bromopropanoic acid **7b** (1.42 g, 9.28 mmol) were added to a tube containing dimethylformamide (DMF,4 mL). The tube was sealed and the mixture stirred at 80 °C for 22 h. Afterwards, the mixture was transferred to a Falcon tube and washed with the following solvents by centrifugation followed by sonication: EtOAc (3 × 20 mL) then Et_2O (2 × 20 mL). The resulting solid was dried under vacuum to give **8b** as a yellow solid (400 mg, 78.7 %). ^{1}H NMR (DMSO-d_6) δ 9.40 – 9.30 (m, 2H), 8.89 (s, 1H), 8.37 – 8.31 (m, 2H), 8.25 (d, J = 8.4 Hz, 2H), 7.66 – 7.59 (m, 2H), 7.59 – 7.46 (m, 4H), 5.02 – 4.91 (m, 2H), 3.26 (t, J = 7.0 Hz, 2H).; ^{13}C{1H}NMR (DMSO) δ 171.7, 155.9, 145.5, 130.6, 130.3, 130.2, 129.1, 128.8, 128.4, 127.2, 125.8, 124.8, 56.2, 34.6.

5-(4-(anthracen-9-yl)pyridin-1-ium-1-yl)pentanoate (8c): **3** (583 mg, 2.28 mmol) and 5-bromopentanoic acid **7c** (2.15 g, 11.9 mmol) were added to a tube containing DMF (4 mL). The tube

was sealed and the mixture stirred at 80 °C for 22 h. Afterwards, the mixture was transferred to a Falcon tube and washed with the following solvents by centrifugation followed by sonication: EtOAc (3 × 20 mL) then Et_2O (2 × 20 mL). The resulting solid was dried under vacuum to give **8c** as a yellow solid (477 mg, 47.9 %). ^{1}H NMR (DMSO-*d6*) δ 9.42 – 9.36 (m, 2H), 8.88 (s, 1H), 8.37 – 8.31 (m, 2H), 8.24 (d, *J* = 8.5 Hz, 2H), 7.64 – 7.51 (m, 6H), 4.81 (t, *J* = 7.4 Hz, 2H), 2.39 (t, *J* = 7.2 Hz, 2H), 2.14 (p, *J* = 7.6 Hz, 2H), 1.70 (p, *J* = 7.3 Hz, 2H); ^{13}C{1H}NMR (DMSO) δ 174.2, 155.6, 145.0, 130.6, 130.5, 130.2, 129.1, 128.8, 128.4, 127.2, 125.8, 125.0, 60.2, 33.0, 30.3, 21.1.

4-(anthracen-9-yl)-1-(2-hydrazinyl-2-oxoethyl)pyridin-1-ium chloride (9a): A solution of **3** (300 mg, 1.18 mmol) and **6** (558 mg, 2.28 mmol) in chloroform (4 mL) was heated at 120 °C for 4 h in a closed vessel. The reaction mixture was washed by repeated centrifugation and sonication with Et_2O:EtOAC (1:1, 35 mL) and then Et_2O (35 mL). The resulting solid was redissolved in DCM (4 mL) to which 4 M HCl in dioxane (4 mL) was added and then stirred at room temperature for 1 h. The reaction mixture was washed by repeated centrifugation and sonication with the following solvents: EtOAc (35 mL), 1:3 IPA:EtOAc (2 × 10 mL), ½ saturated $NaHCO_3$ (2 × 10 mL), H_2O (10 mL) and finally Et_2O (35 mL). The solid product was dried under vacuum to yield **9a** as a brown solid (230 mg, 53.8 %). ^{1}H NMR (DMSO-*d6*) δ 9.38 (d, *J* = 6.7 Hz, 2H), 8.90 (s, 1H), 8.42 (d, *J* = 6.8 Hz, 2H), 8.26 (d, *J* = 8.3 Hz, 2H), 7.68 – 7.52 (m, 4H), 7.48 (d, *J* = 8.6 Hz, 2H), 5.91 (s, 2H); ^{13}C{1H}NMR (DMSO) δ 164.1, 156.8, 146.6, 130.6, 130.3, 129.9, 129.4, 128.9, 128.3, 127.5, 125.9, 124.5, 59.7. HRMS (MALDI-FT ICR) *m*/*z*: $[M+H]^+$ Calcd. for $C_{21}H_{18}N_3O$ 328.14444: Found 328.14499.

4-(anthracen-9-yl)-1-(3-hydrazinyl-3-oxopropyl)pyridin-1-ium chloride (9b): Compound **8b** (356 mg, 1.09 mmol) was added to DCM (20 mL). Oxalyl chloride (390 µL, 4.55 mmol) and DMF (2 drops) were added and the mixture was stirred for 1 h at room temperature. Afterwards, the solvent was evaporated under reduced pressure, a solution of **5** (1.19 g, 9.02 mmol) in DCM (20 mL) was added and the reaction mixture was stirred for 16 h at room temperature. Next, 4 M HCl in dioxane (20 mL) was added and the mixture was stirred at room temperature for a further 23 h. Subsequently, the solvent was evaporated almost to dryness and the residue was washed by repeated centrifugation and sonication with the following solvents: EtOAC (35 mL), 1:3 IPA:EtOAc (2 × 10 mL), ½ saturated

$NaHCO_3$ (2 × 10 mL), H_2O (10 mL) and finally Et_2O (35 mL). The resulting solid was dried under vacuum to yield **9b** as a yellow solid (317, 77.1 %). ^{1}H NMR (DMSO-d_6) δ 11.69 (s, 1H, NH), 9.41 (d, *J* = 6.5 Hz, 2H), 8.88 (s, 1H), 8.33 (d, *J* = 6.5 Hz, 2H), 8.24 (d, *J* = 8.4 Hz, 2H), 7.65 – 7.58 (m, 2H), 7.59 – 7.51 (m, 4H), 5.07 (t, *J* = 6.7 Hz, 2H), 3.28 (t, *J* = 6.6 Hz, 2H); ^{13}C{1H}NMR (DMSO) δ 168.4, 156.0, 145.6, 130.6, 130.4, 130.2, 129.1, 128.8, 128.4, 127.3, 125.8, 124.9, 56.2, 33.8. HRMS (MALDI-FT ICR) *m*/*z*: $[M+H]^+$ Calcd. for $C_{22}H_{20}N_3O$ 342.16009: Found 342.16062.

4-(anthracen-9-yl)-1-(5-hydrazinyl-5-oxopentyl)pyridin-1-ium chloride (9c): Compound **8c** (218 mg, 0.500 mmol) was added to DCM (20 mL). Oxalyl chloride (200 µL, 2.33 mmol) and DMF (2 drops) were added and the mixture was stirred for 1 h at room temperature. Next, the solvent was evaporated under reduced pressure, a solution of **5** (635 mg, 4.80 mmol) in DCM (20 mL) was added and the mixture was stirred for 16 h at room temperature. Afterwards, 4 M HCl in dioxane (20 mL) was added and the mixture was stirred at room temperature for a further 23 h. Subsequently, the solvent was evaporated almost to dryness and the residue was washed by repeated centrifugation and sonication with the following solvents: EtOAC (35 mL), 1:3 IPA:EtOAc (2 × 10 mL), ½ saturated $NaHCO_3$ (2 × 10 mL), H_2O (10 mL) and finally Et_2O (35 mL). The resulting solid was dried under vacuum to yield **9c** as a yellow solid (141 mg, 69.5 %). ^{1}H NMR (DMSO-d_6) δ 9.46 (s, 1H, NH), 9.43 – 9.35 (m, 2H), 8.88 (s, 1H), 8.38 – 8.29 (m, 2H), 8.25 (d, *J* = 8.4 Hz, 2H), 7.71 – 7.44 (m, 6H), 4.80 (t, *J* = 7.4 Hz, 2H), 2.23 (t, *J* = 7.3 Hz, 2H), 2.15 – 2.03 (m, 2H), 1.69 (p, *J* = 7.4 Hz, 2H). ^{13}C{1H}NMR (DMSO) δ 171.1, 155.6, 145.0, 130.6, 130.5, 130.3, 129.1, 128.8, 128.4, 127.2, 125.8, 125.0, 60.1, 32.6, 30.3, 21.7. HRMS (MALDI-FT ICR) *m*/*z*: $[M+H]^+$ Calcd. for $C_{24}H_{24}N_3O$ 370.19139: Found 370.19393.

Animal Experiments and Tissue Preparation

Rat and mouse brain as well as rat adrenal cortex and lung tissue were used for optimisation of the derivatisation conditions and evaluation of the derivatisation efficiency. All tissues were obtained and the animal experiments conducted in agreement with the European Communities Council Directive of November 24, 1986 (86/609/EEC) on the ethical use of animals.

Budesonide-exposed lung tissue from male Wistar rats of approximately 350 g body weight (Taconic, Denmark) was obtained from *in vivo* endotracheal experiments approved by the local ethical committee at Lund/Malmö, Sweden (no. M84-05). Following a 5 day acclimatisation period in a climate-controlled room (12 h light-dark cycle, temperature 22 °C, 55 % humidity) with food and water given *ad libitum*, budesonide was administered to the rats as an aerosol of a nebulised solution in an in-house built two-stage nose-only flow-past inhalation chamber (Battelle Design) [7], resulting in a lung deposited dose of 0.25 mg/kg. The animals were anesthetised and sacrificed 15 minutes after administration, whereupon the lungs were rapidly dissected out.

Rat brain and adrenal tissue was obtained from experiments approved by the local ethical committee at the Karolinska Institute, Stockholm, Sweden (N350/08 and N105/16). Male Sprague-Dawley rats were housed in a controlled environment (12 h light-dark cycle, temperature 20 °C, 53 % humidity). The brains and adrenal glands were rapidly dissected out following euthanasia by decapitation.

Mouse brain tissue was obtained from experiments approved by the local ethical committee at the Karolinska Institute, Stockholm, Sweden (N351/08). Three-month-old male C57Bl/6 mice were housed in an airconditioned room (12 h light-dark cycle, temperature 20 °C, 53 % humidity). The mouse brain was rapidly removed following anesthetisia and euthanasia.

All tissues were frozen with dry-ice-cooled isopentane and stored at −80 °C before further processing.

MALDI Imaging

To evaluate the derivatisation efficiency of the developed matrices, five different amounts in 50 nL of three model compounds (i.e. progesterone, budesonide and fluticasone propionate, SI Fig. S) dissolved in 50 % ethanol were spotted onto control rat brain tissue sections using a BioSpot BT600 (BioFluidix GmbH, Freiburg, Germany) prior to matrix application.

Reactive matrix solutions were prepared by dissolving 10 mg of the synthesised matrices in 5800 µL of 70 % methanol and 200 µL of trifluoroacetic acid (TFA) in glass vials. Following 30 s of ultra-sonification (Ultrasonic cleaner, VWR International, Radnor, PA, U.S.A.), an automated pneumatic

sprayer (TM-sprayer, HTX Technologies LLC, Chapel Hill, NC, U.S.A) was used to spray the reagent over the tissue sections. The nozzle temperature was set at 90 °C and the reagents were pneumatically sprayed horizontally at a flow rate of 80 µL/min (6 psi of N_2) over the slides in twenty passes at a linear velocity of 1100 mm/min with 2 mm track spacing. When applicable, a co-matrix (35 mg/mL DHB in 50 % ACN with 0.2 % TFA) was pneumatically applied (6 psi of N_2) on top of the reactive matrices at a set nozzle temperature of 95 °C and flow rate of 70 µL/min over the slides for six passes in a criss-cross manner at a linear velocity of 1100 mm/min with 2 mm track spacing. The slides were not subjected to any additional incubation. Before analysis, the slides were scanned using an Epson perfection V500 flatbed scanner (Seiko Epson Corporation, Nagano, Japan).

All MALDI–MSI experiments were performed in the positive-ion mode using a MALDI FTICR (solariX 7T 2ω, Bruker Daltonics) mass spectrometer equipped with a Smartbeam II 2 kHz laser. The laser power was optimised before each run and then held constant throughout the MALDI–MSI experiment. At each sampling position, 50–100 shots were used to acquire data over an *m*/*z* range of 150–1500 Da. All the used methods were externally calibrated using red phosphorus and internally calibrated using either the cluster ions ($[M]^+$) of the reactive matrices (at *m*/*z* 328.144439, 342.160089 or 346.191389 for 9a, 9b and 9c, respectively) or higher mass lipids (*m*/*z* 734.569432, 760.585082 or 782.567026) as the lock mass. Tissue sections were analysed in random order to prevent any possible bias arising from variations in the mass spectrometer sensitivity or matrix degradation over time. Spectra were normalised against the root mean square (RMS) of all data points. MSI data was visualised using flexImaging v.4.1 (Bruker Daltonics). Identification of compounds was performed either by 1) including a standard compound in the run, 2) considering the accurate mass together with confirmation of the distribution from literature or by using the AMPP (1-(4-(aminomethyl)phenyl)pyridin-1-ium chloride) derivatisation reagent [8] together with a norharmane matrix, or 3) structural elucidation from MS/MS fragmentation (SI Fig. S, SI Table S1).

Synthetic Pathway

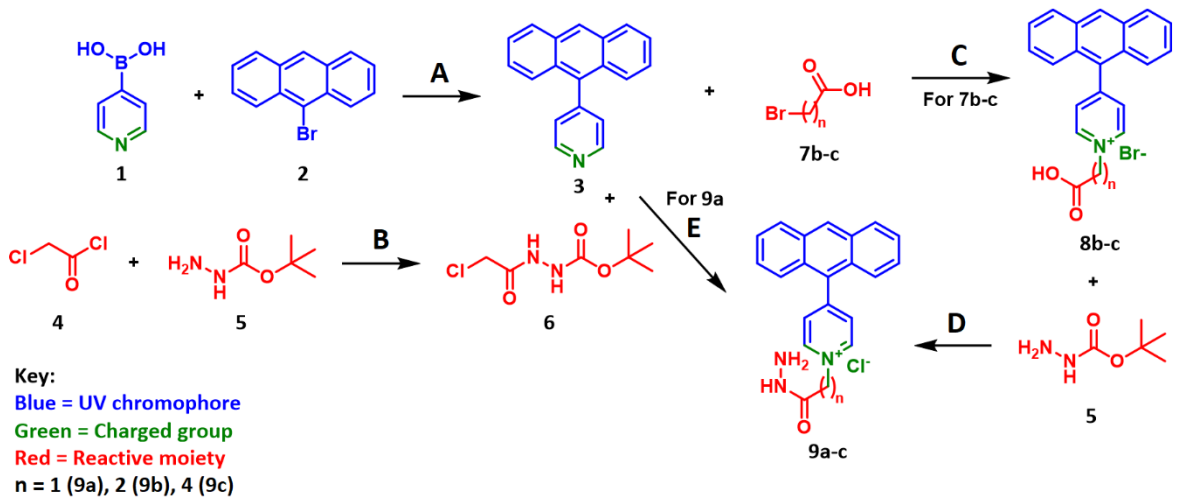

Fig. S1. Synthetic pathway to prepare three reactive matrices (9a-c). Reagents and conditions: (A) $Pd(PPh_3)_4$ (3 mol%), Tol:EtOH:Sat. $NaHCO_3$ (8:2:5), 90 °C, 23 h, 57 %; (B) pyridine, DCM, 0 °C, 6 h, 55 %; (C) DMF, 80 °C, 22 h, 79 % (8b) 48 % (8c); (D) i. oxalyl chloride, 2 drops DMF, $CHCl_3$, rt, 1 h; ii. 5, $CHCl_3$, rt, 16 h; iii. DCM: 4 M HCl in dioxane (1:1), rt, 23 h, 77 % (9b) 70 % (9c) (yield over 3 steps); (E) i. $CHCl_3$, 120 °C, 4 h; ii. DCM: 4 M HCl in dioxane (1:1), rt, 1 h, 54 % (9a) (yield over 2 steps).

Compound ^{13}C and ^{1}H NMR Spectra

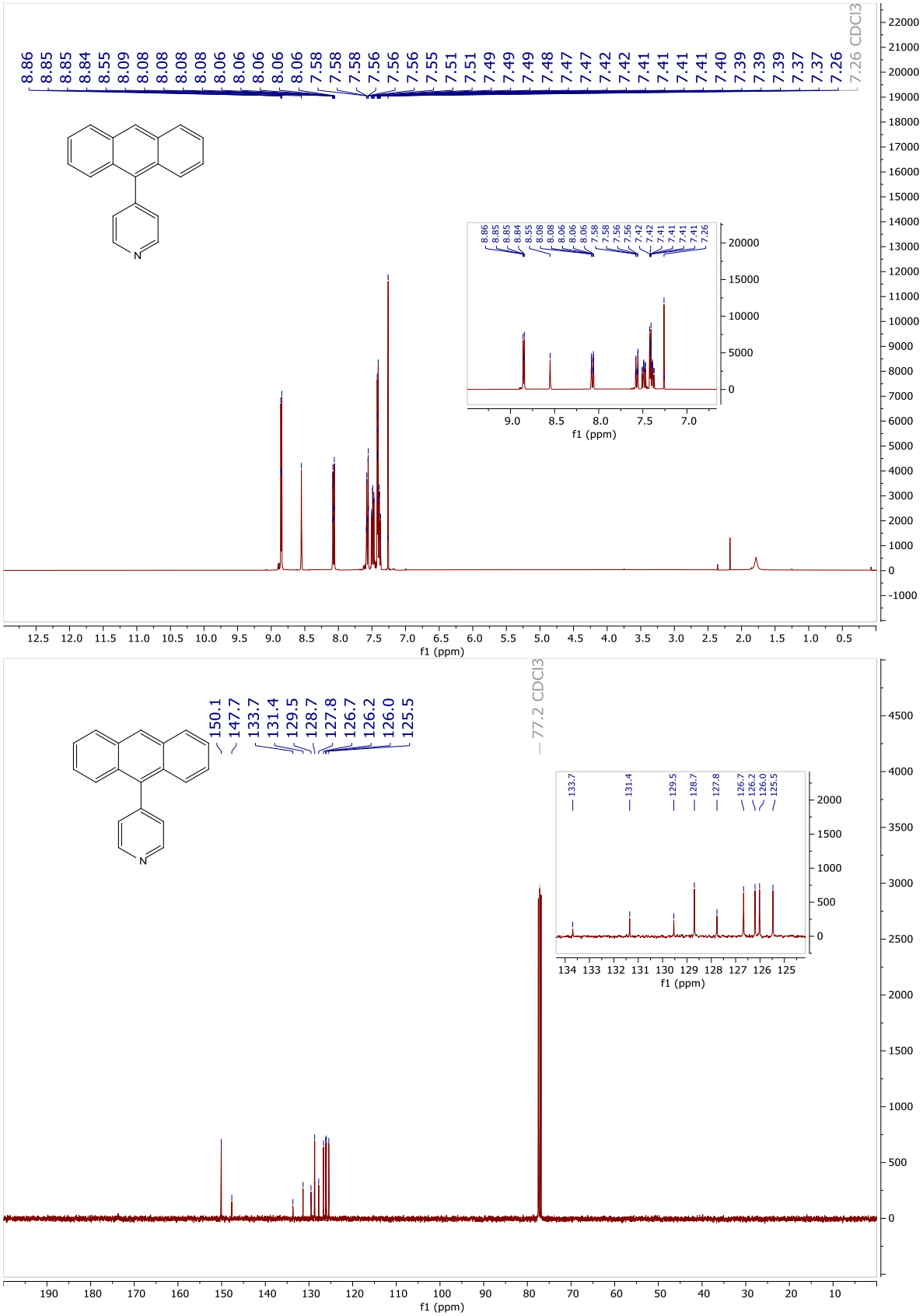

Fig. S2. ^{1}H (400 MHz, CDCl3) (top) and $^{13}C\{1H\}$ (101 MHz, CDCl3) (bottom) NMR spectra of 3.

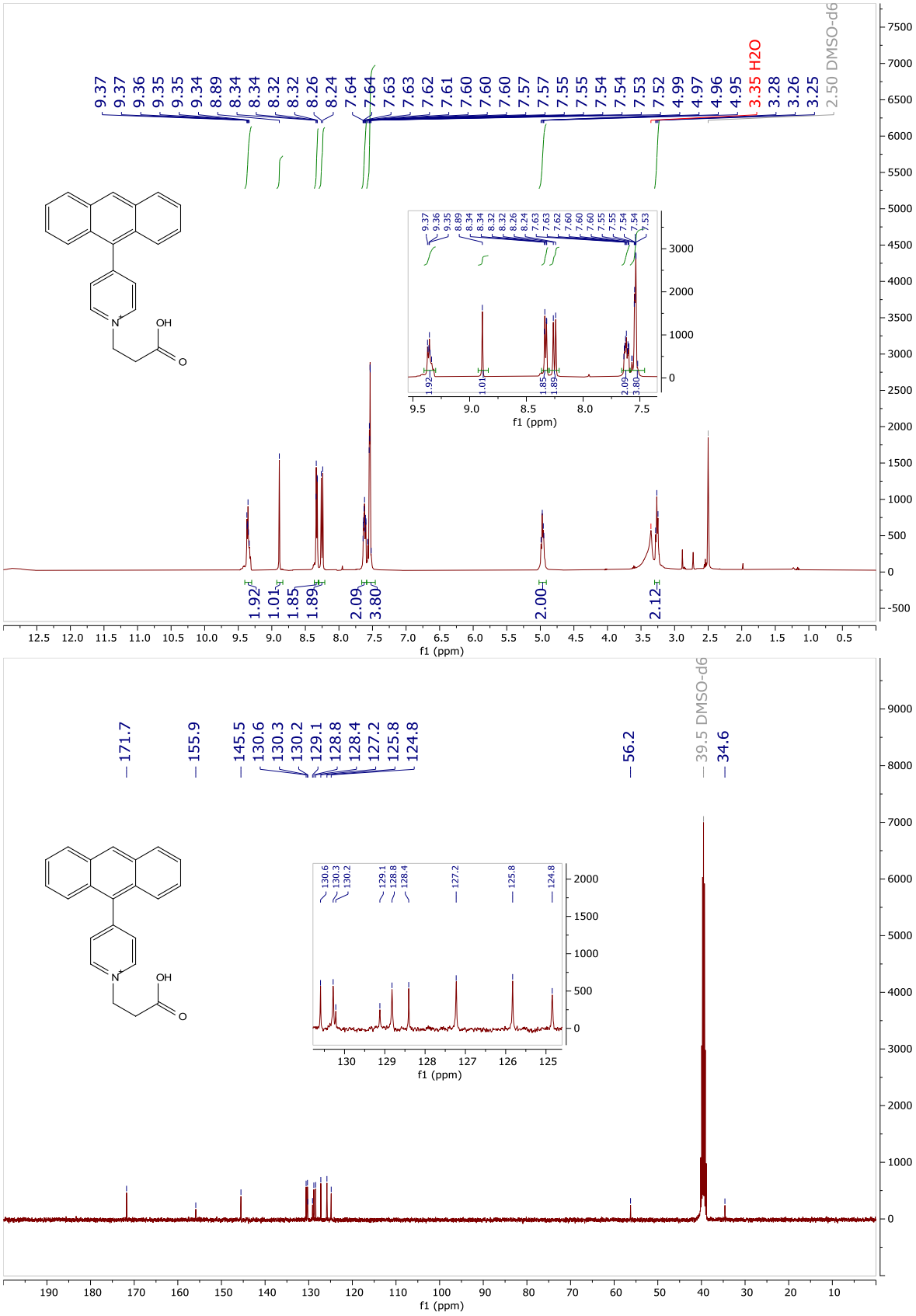

Fig. S3. ^{1}H (400 MHz, DMSO-d6) (top) and ^{13}C{1H} (101 MHz, DMSO) (bottom) NMR spectra of 8b.

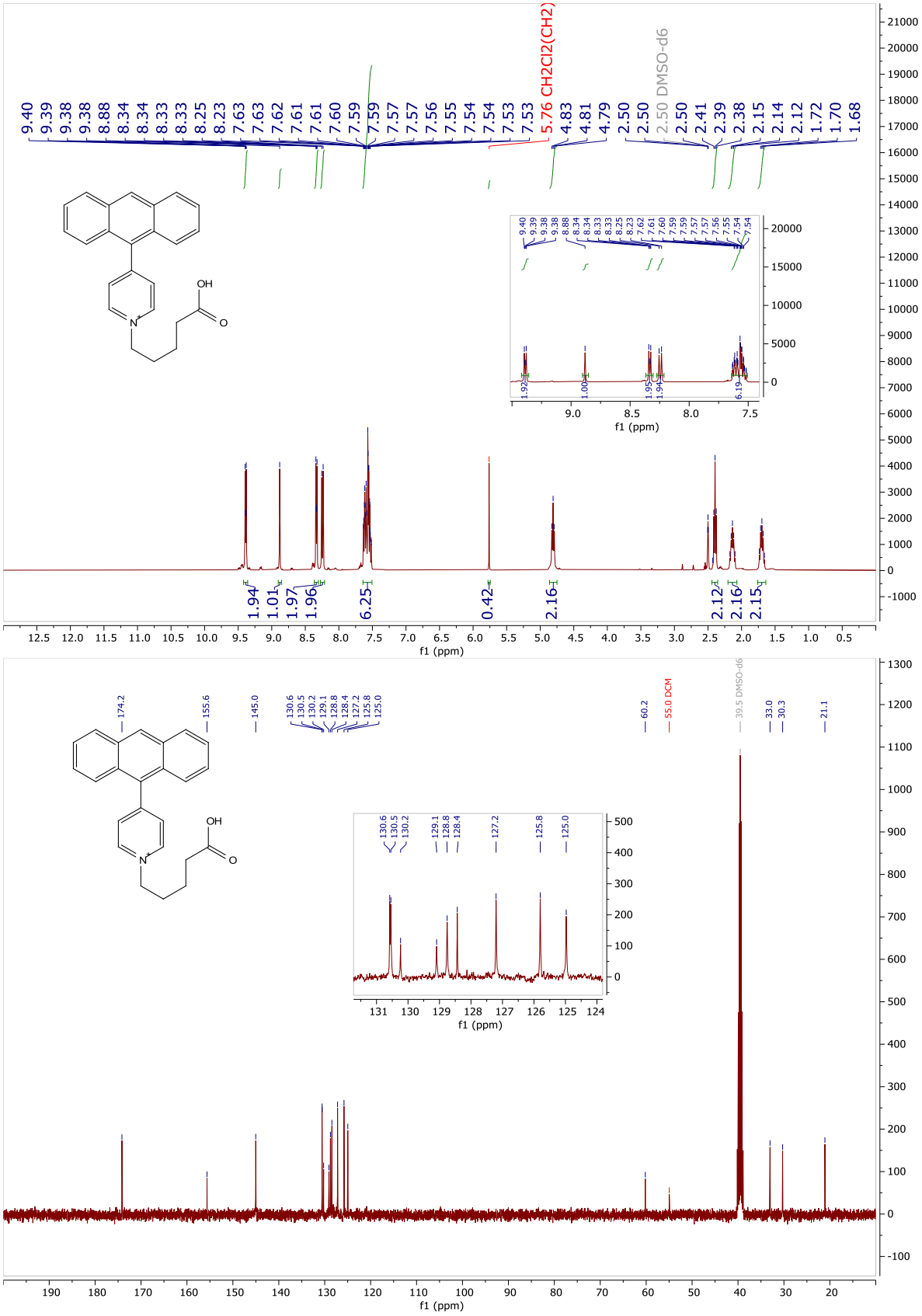

Fig. S4. ^{1}H (400 MHz, DMSO-d6) (top) and ^{13}C{1H} (101 MHz, DMSO) (bottom) NMR spectra of 8c.

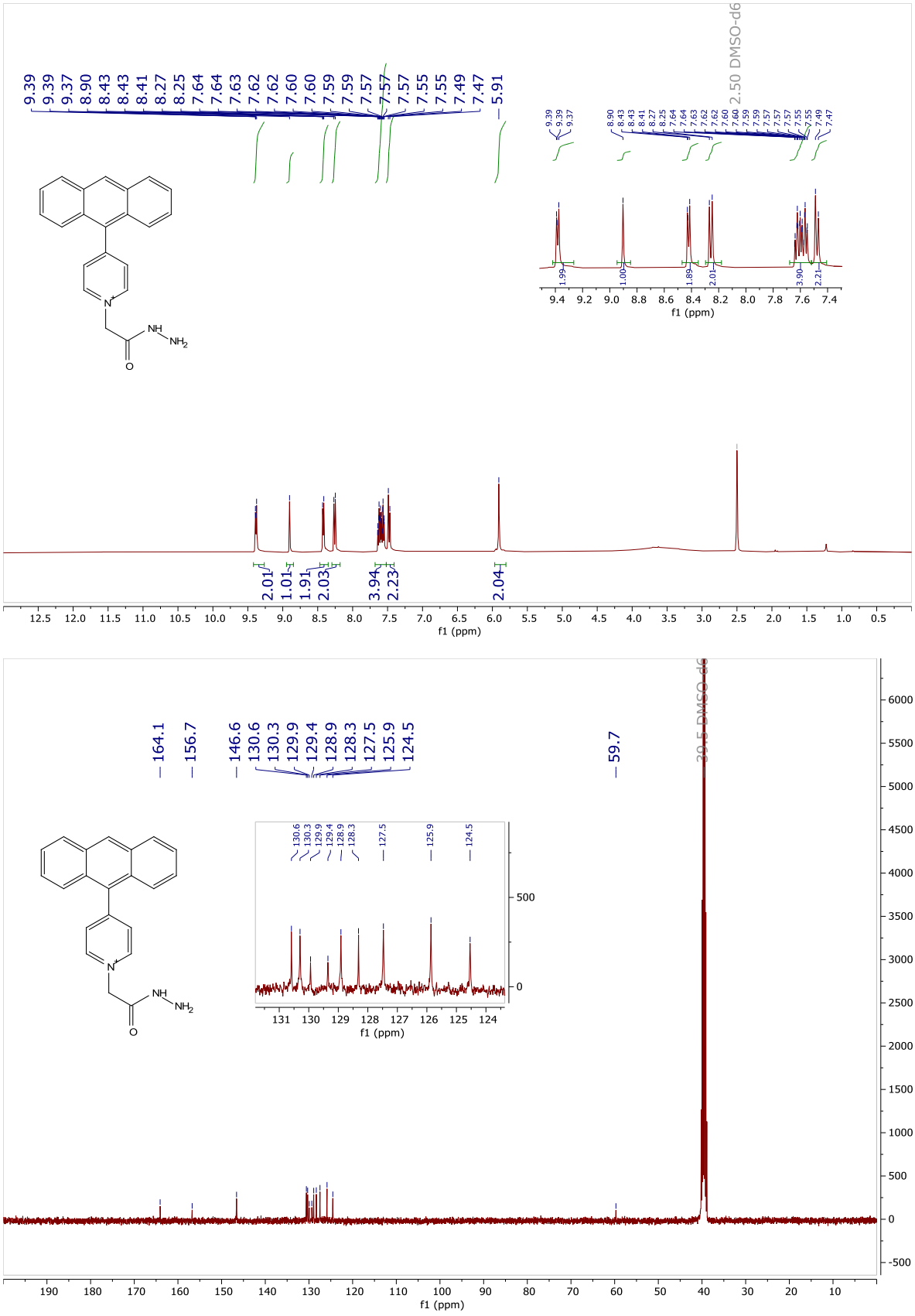

Fig. S5. ^{1}H (400 MHz, DMSO-d6) (top) and ^{13}C{1H} (101 MHz, DMSO) (bottom) NMR spectra of 9a.

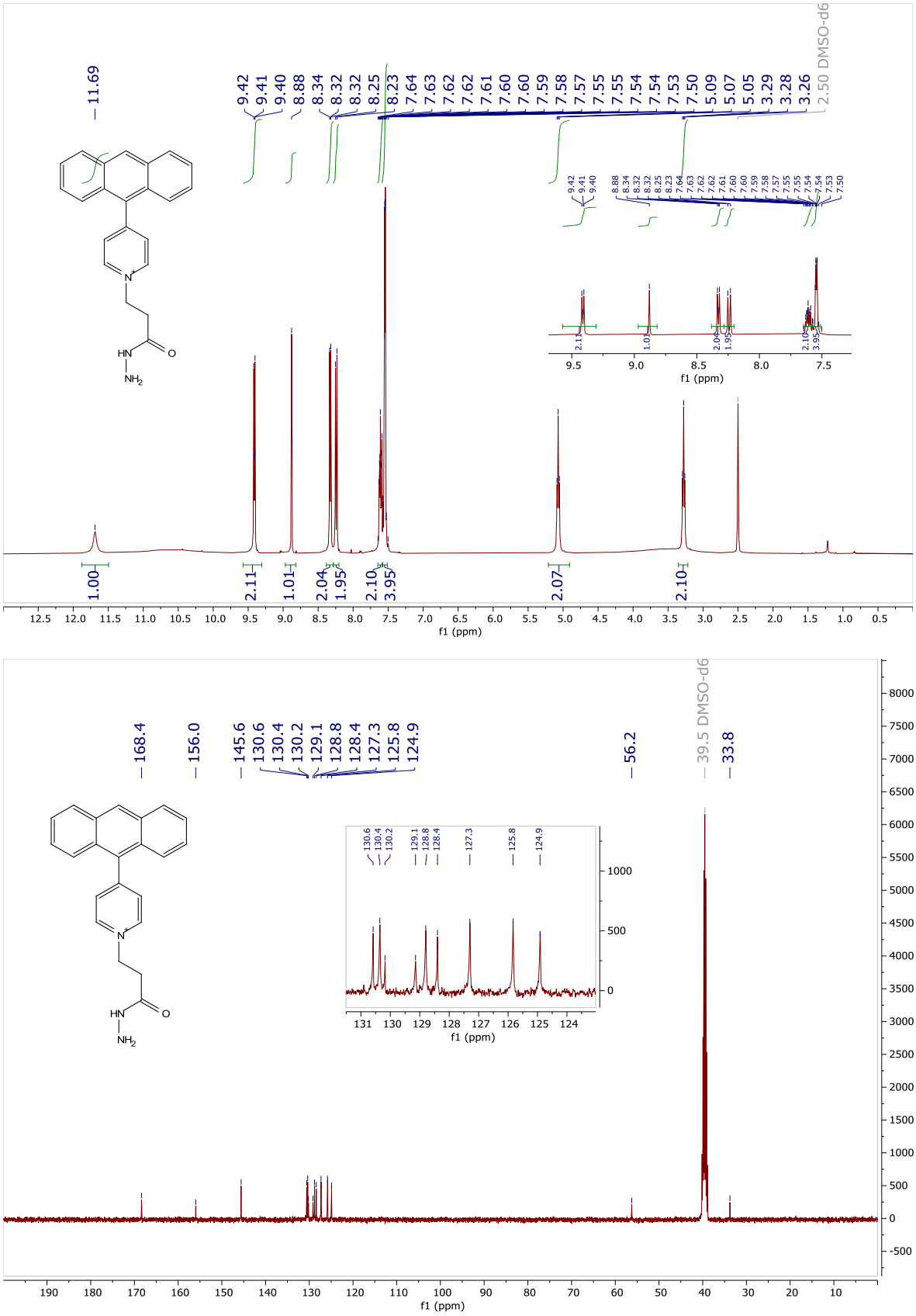

Fig. S6. ^{1}H (400 MHz, DMSO-d6) (top) and ^{13}C{1H} (101 MHz, DMSO) (bottom) NMR spectra of 9b.

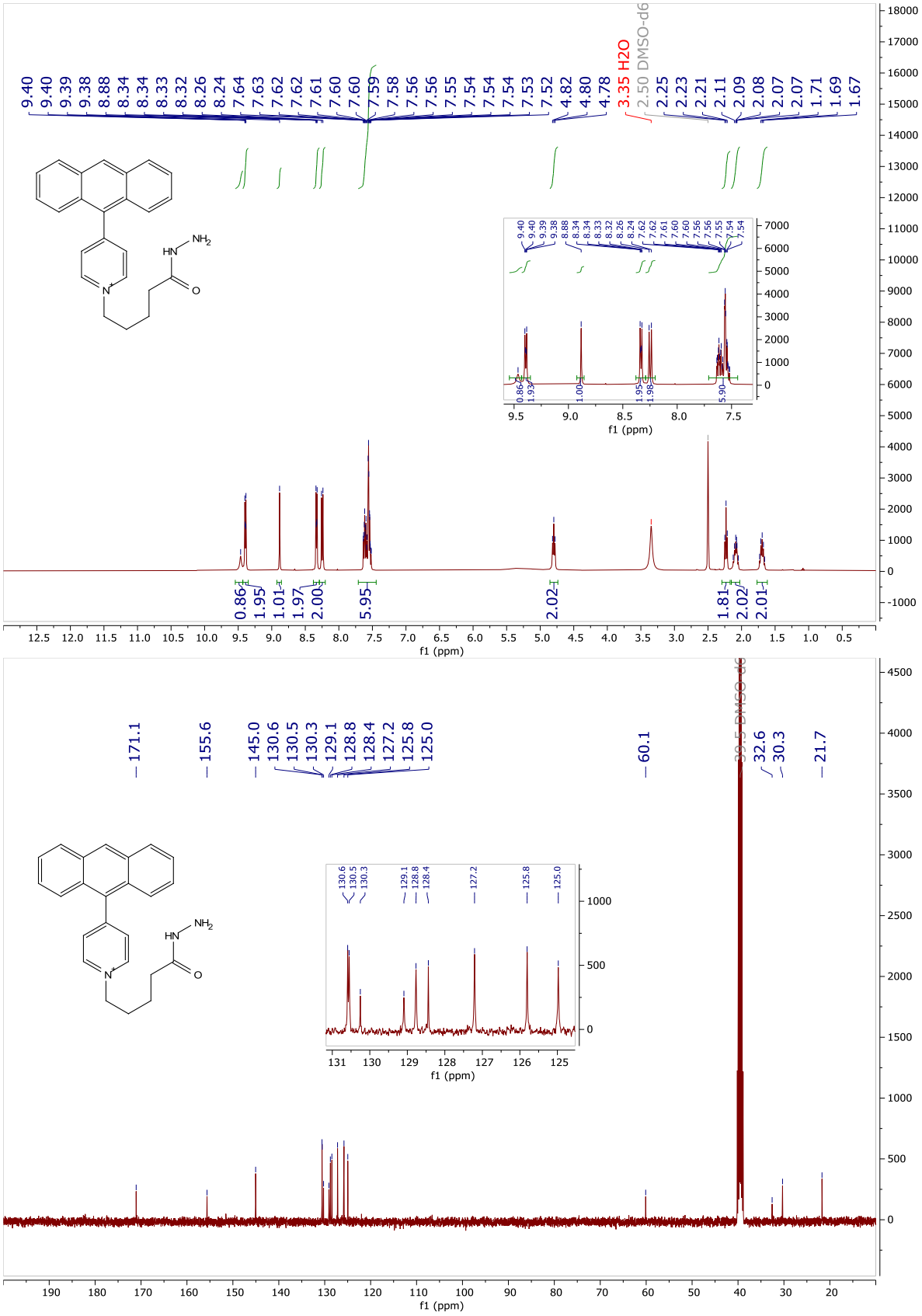

Fig. S7. ^{1}H (400 MHz, DMSO-d6) (top) and ^{13}C{1H} (101 MHz, DMSO) (bottom) NMR spectra of 9c.

Compound UV Spectra

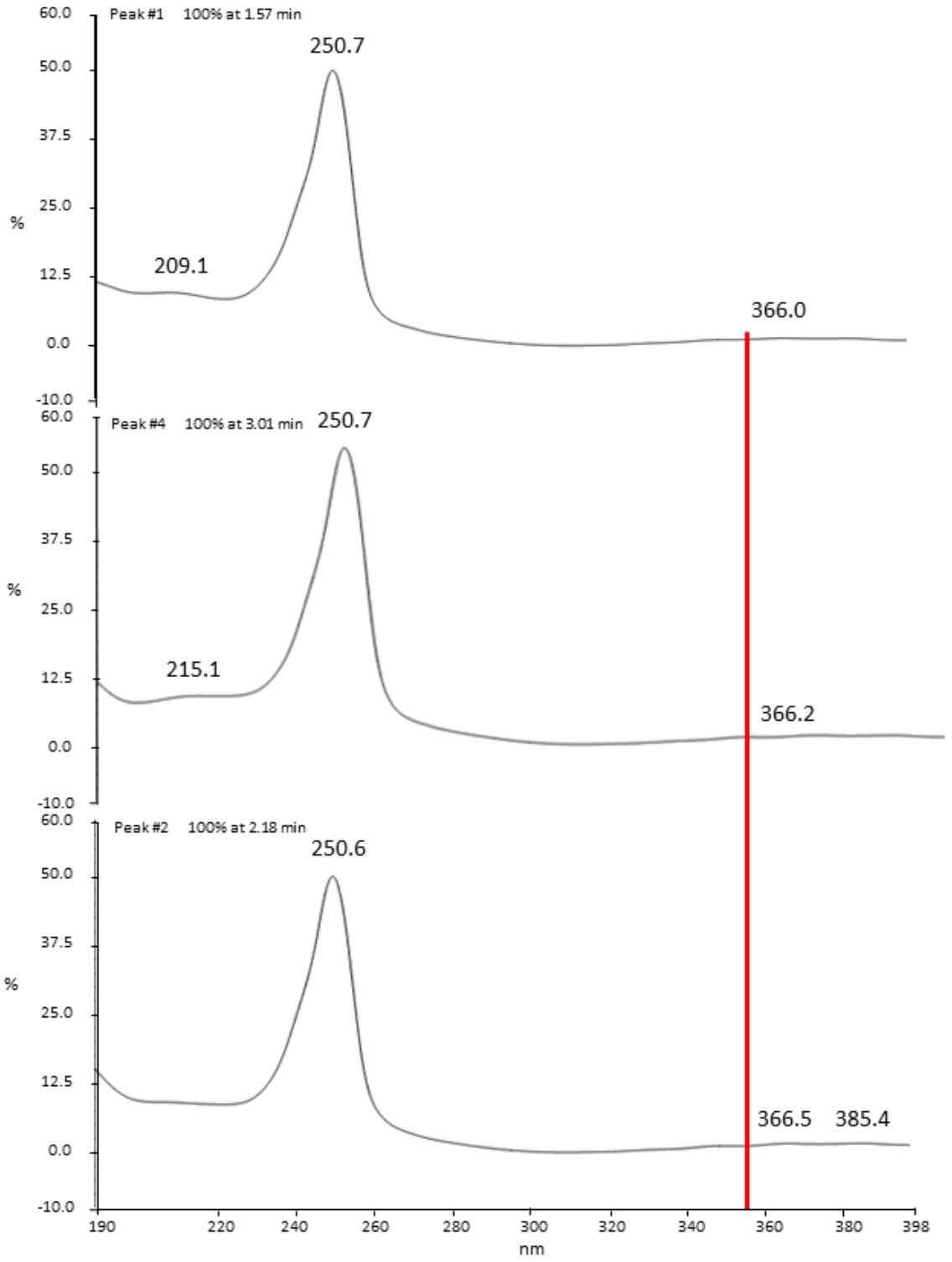

Fig. S8. UV-spectra of reactive matrices 9a-c (from top to bottom). The MALDI laser wavelength (355 nm) is highlighted with a red line through the spectra.

Accurate Mass Determination

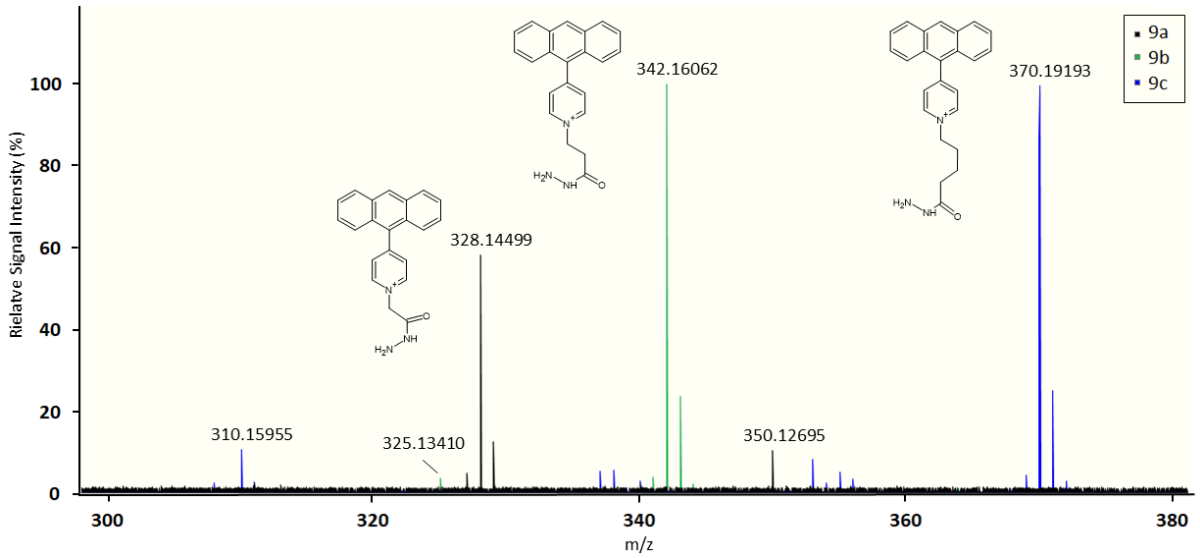

Fig. S9. Accurate mass determination of the reactive matrices. (A) Matrix **9a**: calculated for $C_{21}H_{18}N_3O$ 328.14444, found 328.14499 (+1.7 ppm). (B) Matrix **9b**: calculated for $C_{22}H_{20}N_3O$ 342.16009, found 342.16062 (+1.5 ppm). (C) Matrix **9c**: calculated for $C_{24}H_{24}N_3O$ 370.19139, found 370.19193 (+1.5 ppm).

Model Compound Structures

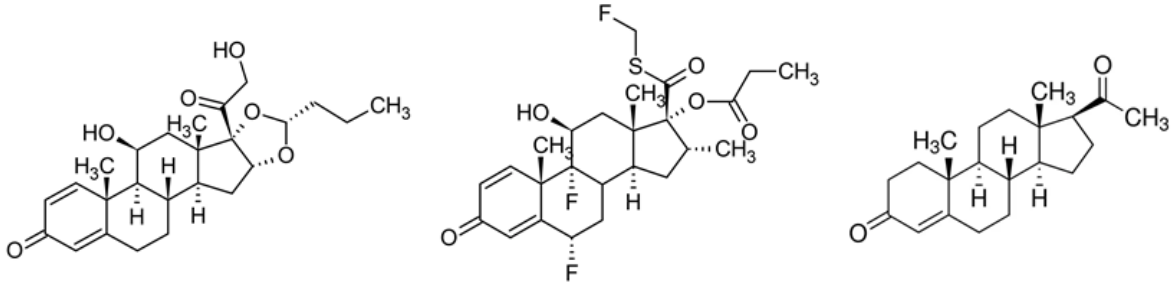

Fig. S10. Structures of the model compounds budesonide, fluticasone propionate and progesterone (from left to right).

MALDI MSI

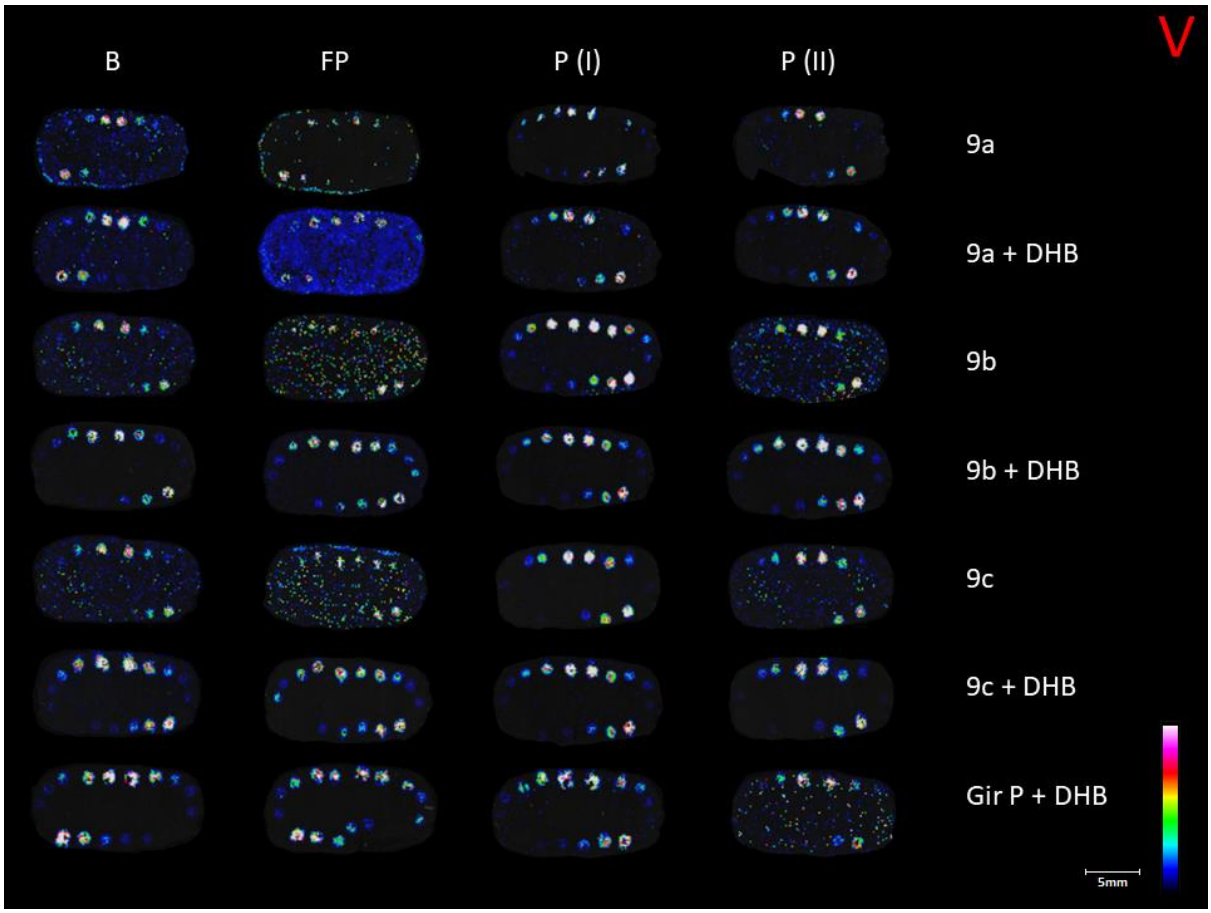

Fig. S11. Ionisation efficiency of reactive matrices (9a-c) vs. Girard's reagent P (Gir P) without and with DHB as a co-matrix. Spotted model compound standards (3x) on rat brain tissue sections: B = budesonide (0.2-8.7 pmol), FP = fluticasone propionate (0.2-7.5 pmol), P = progesterone (0.3-11.9 pmol. Singly derivatised progesterone and doubly derivatised progesterone are denoted by (I) and (II), respectively). Spatial resolution = 150 µm (small laser focus) with 100 shots per raster position. RMS-normalised data. The intensity was set individually to reveal as many spots as possible with the different matrices. An insufficient signal was obtained with Gir P without co-matrix (data not shown). For additional information, see the experimental section.

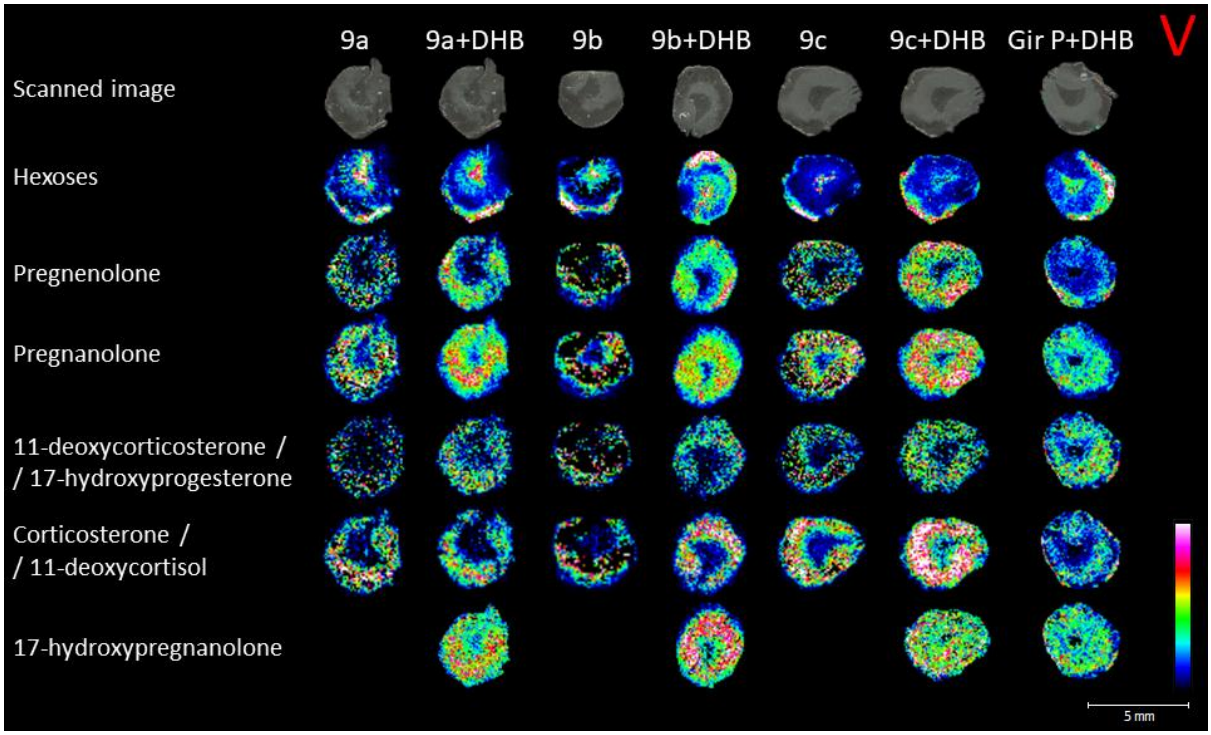

Fig. S12. Imaging of endogenous compounds in rat adrenal cortex with reactive matrices (9a-c) vs. Girard's reagent P (Gir P) without and with DHB as a co-matrix. Spatial resolution = 80 µm (small laser focus) with 100 shots per raster position. RMS-normalised data. The intensity was set individually to reveal the best possible distribution with the different matrices. An insufficient signal was obtained with Gir P without co-matrix (data not shown). For additional information, see the experimental section.

MS/MS Spectra

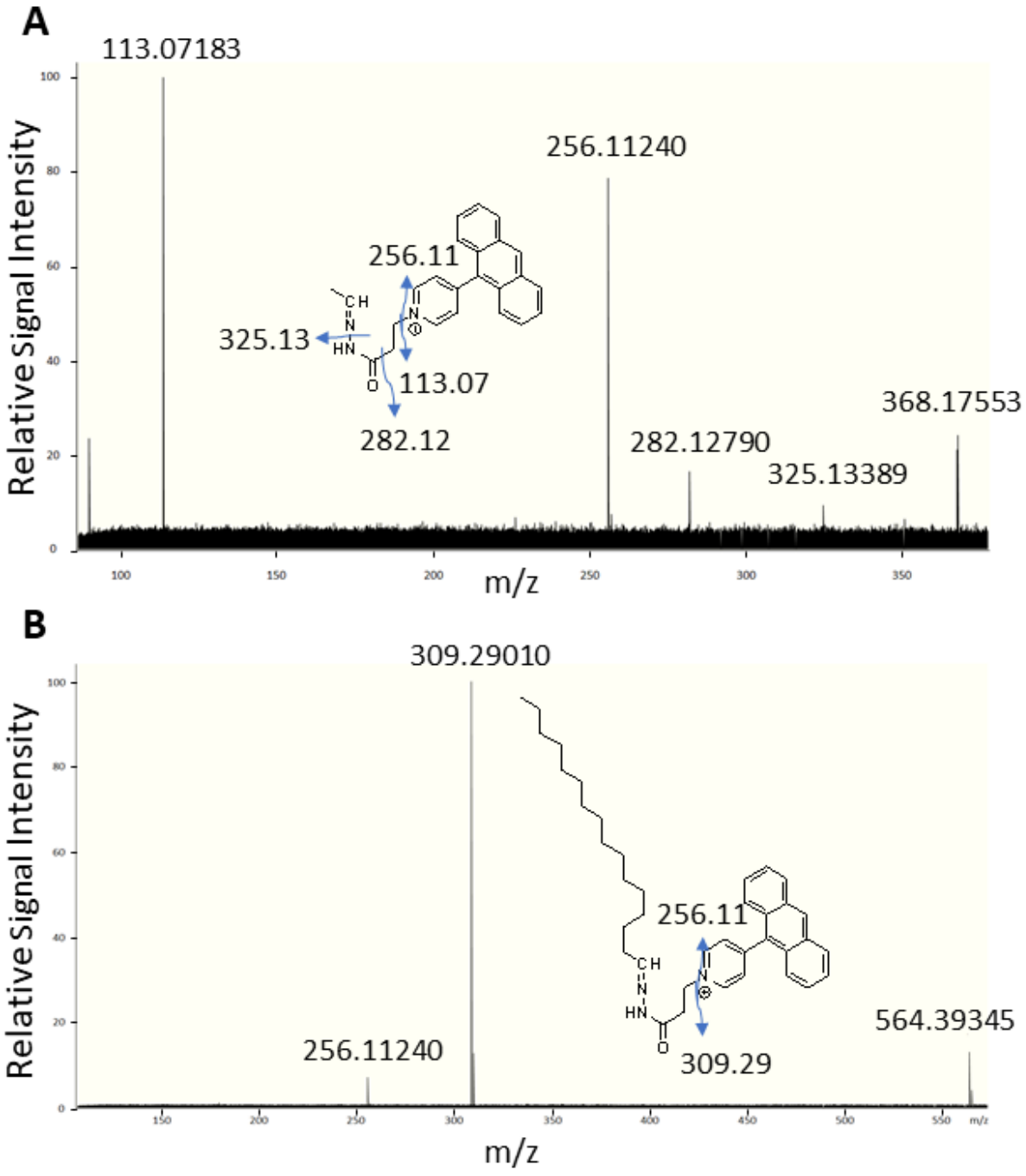

Fig. S13. MS/MS spectra obtained from rat brain tissue sections using MALDI-CID-FTICR from the matrix 9b-derivatised precursor ions. Proposed fragmentation pathways for **9b**-derivatised acetaldehyde, *m/z* 368.175 (A) and hexadecanal, *m/z* 578.411 (B). Since the isolation window width was 1 *m/z* unit for hexadecanal, isobaric and isomeric compounds may also have been fragmented, giving rise to additional product ions.

High-resolution imaging

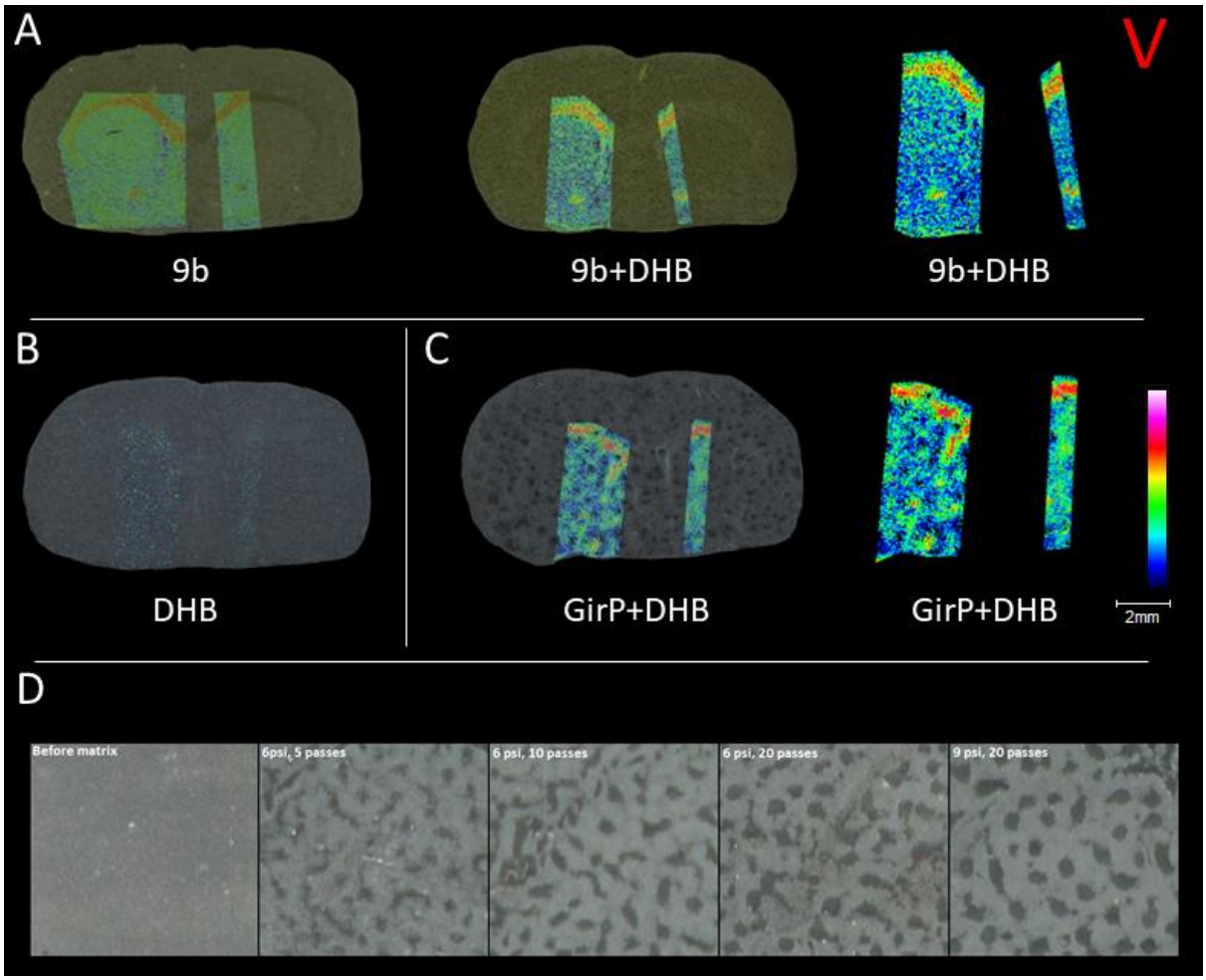

Fig. S14. High spatial resolution imaging of heptadecanal in rat brain. (A) Imaging with reactive matrix **9b** (with and without DHB co-matrix) at *m/z* 578.4103 $[M+9b-H_2O]^+$. (B) Imaging with DHB alone at *m/z* 255.2683 $[M+H]^+$. (C) Imaging with Girard's reagent P (Gir P) with DHB as co-matrix at *m/z* 388.3325 $[M+GirP-Cl-H_2O]^+$. Spatial resolution: 40 µm (left, larger region) and 20 µm (right, smaller region). 9 psi N_2 pressure during matrix application. 50 shots per raster position (small laser focus). RMS-normalised data. The intensity was set individually to reveal the best possible distribution of the compound. (D) Repeated matrix application test for elucidation of holes appearing in the tissue upon application of Gir P matrix. Scanned images (left to right): tissue before matrix application → after 5 passes at 6 psi N_2 → after 10 passes at 6 psi N_2 → after 20 passes at 6 psi N_2 → after 20 passes at 9 psi N_2. For additional information, see the experimental section.

Supporting Tables

Table S1. Sensitivity (LOQ) and linearity data (R^2) for model compounds spotted on rat brain using different matrices. Applied amounts of standards (within 50 nL, *n* = 3): budesonide 0.19, 0.30, 0.92, 2.83 and 8.72 pmol; fluticasone propionate 0.16, 0.26, 0.79, 2.44 and 7.50 pmol; progesterone 0.26, 0.41, 1.26, 3.88 and 11.9 pmol. Single derivatised progesterone and double derivatised progesterone are denoted by (I) and (II), respectively. The LINEST-function in MS Excel 2019 was used to analyse line statistics used for calculation of the limits of quantification (LOQ) as 10 × SD *Y*-intercept / slope. Coefficients of determination (R^2) are given within brackets.

Matrix	Budesonide	Fluticasone propionate	Progesterone (I)	Progesterone (II)
9a	1.8 pmol (0.9944)	0.2 pmol (0.9993) [a]	0.2 pmol (1.0000) [d]	0.9 (0.9995) [e]
9a + DHB	1.9 pmol (0.9941)	1.2 pmol (0.9980) [a]	1.2 pmol (0.9992) [d]	1.1 (0.9993) [e]
9b	2.1 pmol (0.9920)	1.2 pmol (0.9992) [b]	2.7 pmol (0.9935)	1.7 (0.9986) [f]
9b + DHB	0.7 pmol (0.9991)	0.1 pmol (0.9998) [a]	0.5 pmol (0.9998)	0.4 (0.9999)
9c	1.5 pmol (0.9962)	1.4 pmol (0.9914) [c]	1.3 pmol (0.9984)	1.5 (0.9979)
9c + DHB	0.3 pmol (0.9998)	0.3 pmol (0.9990) [a]	1.1 pmol (0.9988)	1.0 (0.9995) [f]
Gir P	N.R.	N.R.	N.R.	N.R.
Gir P + DHB	1.7 pmol (0.9952)	0.6 pmol (0.9957) [a]	0.1 pmol (0.9999) [e]	3.7 (0.9932) [f]

Excluded standards in order to improve curve fit: [a] no. 5 (7.50 pmol), [b] no. 1 (0.16 pmol) and no. 4 (2.44 pmol), [c] no. 1 (0.16 pmol) and no. 5 (7.50 pmol), [d] no. 4 (3.88 pmol), [e] no. 5 (11.9 pmol), [f] no. 1 (0.26 pmol). N.R. = no results (i.e. no visible standard spots).

Table S2. Identification of metabolites in mouse and rat brain tissue sections following derivatisation with reactive matrix 9b. The neurotransmitter metabolite 3,4-dihydroxyphenylacetaldehyde (DOPAL) and monosaccharides (pentoses and hexoses) were determined based on the mass accuracy and known specific distribution within brain tissue sections [7]. Aldehyde species, including fatty aldehydes, were identified by comparison with the known distribution using an aldehyde reactive matrix (AMPP) together with norharmane as co-matrix [7] and by MS/MS fragmentation, indicating that they had been derivatised with matrix **9b**. MS/MS data for metabolites were obtained directly from mouse and/or rat brain tissue sections (Supporting Information Fig. S13). However, additional isobaric and isomeric compounds may also have been fragmented within the same MS/MS analysis.

Metabolite	Formula	M	M+H	M+9b formula	M+9b theoretical	Brain	M+9b observed	Mass error (ppm)
Acetaldehyde	C2H4O	44.02622	45.03349	C24H22N3O	368.17574	Mouse	368.17559	-0.4
						Rat	368.17558	-0.4
DOPAL	C8H8O3	152.04734	153.05462	C30H26N3O3	476.19687	Mouse	476.19666	-0.4
Pentose	C5H10O5	150.05282	151.06010	C27H28N3O5	474.20235	Mouse	474.20204	-0.6
						Rat	474.20241	0.1
Hexose	C6H12O6	180.06339	181.07066	C28H30N3O6	504.21291	Mouse	504.21325	0.7
						Rat	504.21298	0.1
Hexadecanal	C16H32O	240.24532	241.25259	C38H50N3O	564.39484	Mouse	564.39485	0.0
Heptadecanal *	C17H34O	254.26097	255.26824	C39H52N3O	578.41049	Mouse	578.41059	0.2
Octadecenal *	C18H34O	266.26097	267.26824	C40H52N3O	590.41049	Mouse	590.41023	-0.4
						Rat	590.41034	-0.3
Octadecanal *	C18H36O	268.27662	269.28389	C40H54N3O	592.42614	Mouse	592.42633	0.3
						Rat	592.42595	-0.3

[*] If there were multiple primary hits for a molecule following identification based on accurate mass, the compound with the highest probability of a specific brain distribution was selected.

References

1 A. Girard and G. Sandulesco, *Helv. Chim. Acta,* 1936, **19**, 1095-1107.
2 W. J. Griffiths, S. Liu, G. Alvelius and J. Sjövall, *Rapid Commun. Mass Spectrom.,* 2003, **17**, 924-935.
3 M. Schumacher, S. Weill-Engerer, P. Liere, F. Robert, R. J. Franklin, L. M. Garcia-Segura, J. J. Lambert, W. Mayo, R. C. Melcangi, A. Parducz, U. Suter, C. Carelli, E. E. Baulieu and Y. Akwa, *Prog. Neurobiol.,* 2003, **71**, 3-29.
4 Y. Sugiura, E. Takeo, S. Shimma, M. Yokota, T. Higashi, T. Seki, Y. Mizuno, M. Oya, T. Kosaka, M. Omura, T. Nishikawa, M. Suematsu and K. Nishimoto, *Hypertension,* 2018, **72**, 1345-1354.
5 Y. Wang and W. J. Griffiths, *Neurochem. Int.,* 2008, **52**, 506-521.
6 M. Shariatgorji, A. Nilsson, E. Fridjonsdottir, T. Vallianatou, P. Källback, L. Katan, J. Sävmarker, I. Mantas, X. Zhang, E. Bezard, P. Svenningsson, L. R. Odell and P. E. Andrén, *Nat. Methods,* 2019, **16**, 1021-1028.
7 M. Dahlbäck and S. Eirefelt, *Edinburgh. Ann. Occup. Hyg.,* 1994, **Inhaled particles VII**, 127–134.
8 I. Kaya, L. S. Schembri, A. Nilsson, R. Shariatgorji, S. Baijnath, X. Zhang, E. Bezard, P. Svenningsson, L. R. Odell and P. E. Andrén, *J. Am. Soc. Mass Spectrom.,* 2023, **34**, 836-846.